Original Article

Feasibility study of robotic hypofractionated lung radiotherapy by individualized internal target volume and XSight Spine Tracking: A preliminary dosimetric evaluation

ABSTRACT

Aim: To investigate the dosimetric impacts of lung tumor motion in robotic hypofractionated radiotherapy for lung cancers delivered through continuous tracking of the vertebrae by the XSight Spine Tracking (XST) mode of the CyberKnife.

Materials and Methods: Four-dimensional computed tomography (4DCT) scans of a dynamic thorax phantom were acquired. Three motion patterns (one-dimensional and three-dimensional) of different range were investigated. Monte Carlo dose distributions were generated with 4DCT-derived internal target volume (ITV) with a treatment-specific setup margin for 12.6 Gy/3 fractions. Six-dimensional error correction was performed by kV stereoscopic imaging of the phantom's spine. Dosimetric effects of intrafractional tumor motion were assessed with Gafchromic films (Ashland Inc, Wayne, NJ, USA) according to 1) the percent measurement dose points having doses above the prescribed ($P_{>Dpres}$), mean ($P_{>Dm}$), and minimum ($P_{>Dmin}$) ITV doses, and 2) the coefficient of variation (CV).

Results: All plans attained the prescription dose after three fractions despite marked temporal dose variations. The value of $P_{>Dpres}$ was 100% after three fractions for all plans, but could be smaller (~96%) for one fraction. The values of $P_{>Dmin}$ and $P_{>Dm}$ varied drastically interfractionally (25%-2%), and could be close to 0% after three fractions. The average CV ranged from 2.8% to 7.0%. Correlations with collimator size were significant for $P_{>Dmin}$ and $P_{>Dm}$ ($P < 0.05$) but not $P_{>Dpres}$ ($P > 0.05$).

Conclusions: Treating lung tumors with CyberKnife through continuous tracking of the vertebrae should not be attempted without effective means to reduce the amplitude and variability of target motion because temporal dose variations owing to the intrafractional target motion can be significant.

KEYWORDS: CyberKnife, hypofractionated stereotactic lung radiotherapy, intrafractional organ motion, tracking

Mark K.H. Chan, Dora L.W. Kwong[1], Venus W.Y. Lee, Ronnie W.K. Leung, Mathew Y.P. Wong, Oliver Blanck[2]

Department of Clinical Oncology, Tuen Mun Hospital, Tuen Mun, Hong Kong, [1]Department of Clinical Oncology, The University of Hong Kong, Hong Kong, [2]Department of Radiation Oncology, University Clinic of Schleswig-Holstein, Germany

For correspondence:
Mr. Mark K.H. Chan, Department of Clinical Oncology, Tuen Mun Hospital, Tuen Mun, Hong Kong.
E-mail: ckh456@ha.org.hk

INTRODUCTION

Recently, CyberKnife (Accuray Inc., Sunnyvale, CA, USA), a robotic-based radiosurgical system, has been increasingly employed for stereotactic body radiotherapy (SBRT) of lung cancers.[1,2] Unlike conventional linac-based SBRT, CyberKnife mainly involves non-isocentric and non-coplanar irradiation by a large of small photon beams.

The CyberKnife offers two solutions for treating mobile lung tumors, either by Fiducial Tracking which requires radiopaque fiducial markers to be implanted in or near the tumor,[1] or by XSight Lung Tracking (XLT) which uses the tumor shape for tracking and is hence fiducial free.[3] Both target tracking methods could be combined with the Synchrony real-time respiratory tracking system (RTS).[4] The technical basis of the RTS is a correlation model between an external breathing signal and internal target positions determined from stereoscopic x-ray imaging of the implanted fiducials or the tumor combined with the compensation of that motion by the robotic arm.

The RTS is most suitable for strong moving tumors because the gain in safety margin reduction is proportional to the range of target motion. But for tumors that are attached to rigid structures such as the spinal column and chest wall and that exhibit a small range of motion, fiducial-based RTS may become unjustified considering the additional risks of pneumothorax[5] and fiducial migration[6]. Furthermore, smaller intra-and interfractional variability of the tumor baseline position was observed with smaller tumor-to-vertebrae distance.[7,8] The XLT method, on the other hand, is not applicable to all lung tumors as not all

Access this article online

Website: www.cancerjournal.net

DOI: 10.4103/0973-1482.138220

Quick Response Code:

tumors are visible on the x-ray images due to size and location. Alternatively, the XSight Spine tracking (XST),[9] an offline setup correction strategy that is originally intended for tracking vertebral anatomy in SBRT for spine tumors, may be applied. Such treatment setup strategy coincides in concept with the recently available lung optimized treatment option, called 0-view tracking mode, which utilizes the XST of adjacent vertebrae for global patient alignment. Compared to megavoltage (MV) electronic portal imaging device, kilovoltage (kV) stereoscopic imaging with the XST system offers superior image quality of bony anatomy for accurate auto-registration with the digitally reconstructed radiographs (DRRs). Because XST is not capable of tumor motion tracking and does not account for the interfractional and intrafractional uncertainties of the tumor positions larger safety margin is needed compared to the real-time correction by direct tumor detection.

Similar to non-gated treatments, XST requires an internal target volume (ITV) to account for the effect of the semi-periodic respiration induced organ motion. When a large number of small photon beams are combined to dose paint the tumor volume, it often assumes that the tumor moves within a spatially invariant dose cloud. Clearly, as the tumor moves in and out of the radiation fields following the respiratory motion, the delivered dose to each voxel of the tumor may not add up to its expected total dose. As shown in a landmark study by Bortfeld *et al.*,[10] the dose variance introduced by tumor motion depends on the delivery technique because of the arbitrary respiratory phase. The dosimetric impacts of the intrafractional target motion have been experimentally investigated in conventional linac-based isocentric irradiation by Richter *et al.*[11] for single beam, by Nakamura *et al.* and Huang *et al.* for coplanar and noncoplanar conformal radiotherapy,[12,13] by Jiang *et al.*[14] for sliding and step-and-shot intensity-modulated radiotherapy (IMRT), and Ong *et al.* for volumetric arc radiotherapy.[15] On the contrary, our group has performed experimental investigations of the intrafractional target motion for the CyberKnife focusing on the RTS.[16,17] While it is hypothesized that XST based lung tumor treatment may be beneficial for a subset of patients who are medically inoperable, unsuitable for invasive fiducial implantation and whose tumors are not visible on the x-ray tracking system or attached to the vertebral column with limited motion range, experimental evaluations of this delivery technique have never been reported despite its increasing clinical applications.[18-20] In this study, we aimed to evaluate the adequacy of using the XLS-based strategy by studying the dose delivered to a moving tumor. Experimental measurements were made with Gafchromic films placed inside a thorax phantom with a moving tumor substitute.

MATERIALS AND METHODS

Motion phantom setup

The dynamic thorax phantom (CIRS Inc., Norfolk, VA, USA) used in this experimental study consisted of a moving spherical target with film inserts that can accommodate Gafchromic films (Ashland Inc., Wayne, NJ, USA) in coronal and axial planes. For our study we used EBT2 film. The tumor substitute has a density of 1.06 g/cc and was embedded in the center of the spherical target. The phantom was programmed to move the target in a fixed period of 4s and at variable amplitudes: #1) 10mm in the superior-inferior (SI) direction, #2) 20 mm in the SI, 5 mm in the anterior-posterior (AP), and 2 mm in the lateral (LR) direction, and #3) 10 mm in the SI, 5 mm in the AP, and 2 mm in the LR direction. The motion parameters were chosen according to the analysis of our institution that most tumors exhibited motion principally in the SI direction (mean = 8 mm) and less in the AP direction (3 mm) and the LR direction (1 mm). A large motion range of 20 mm was also included as an extreme scenario. The maximum distance between the target's center and the phantom's spine was 6.5 cm. Constant motion was assumed in four-dimensional computed tomography (4DCT) simulation and treatment deliveries.

4DCT simulation, target definition and ITV-to-PTV margin determination

4DCT images of 1.25mm thickness were acquired on a GE Light Speed 64-slice computed tomography scanner (General Electric Company, Waukesha, WI, USA) together with the real-time position management system (RMP, Varian Medical Systems, Palo Alto, CA, USA). The 4DCT dataset was then sent to the Advantage Workstation (General Electric Company, Waukesha, WI, USA) for post-processing using the Advantage 4DCT software. For each 4DCT dataset, 10 equally time-binned three-dimensional computed tomography (3DCT) datasets were created, with the 0% image dataset and the 50% image dataset roughly corresponding to the end-inhale phase and end-exhale phase in the respiratory cycle. Additionally, we created two reconstructed datasets using maximum-intensity projection (MIP) and average-intensity projection (AVG). The MIP and AVG created 3DCT images that represented the greatest and average voxel intensity values throughout the 4DCT dataset, respectively.

Both the MIP and the AVG datasets were imported into the Multiplan v. 4.0.x (Accuray Inc., Sunnyvale, CA, USA) treatment planning system (TPS). The ITV was produced as the union of the simulated gross tumor volume (GTV) over the motion trajectory on the MIP images. Margins from the ITV to the planning target volume (PTV) were calculated according to the Wolthaus *et al.*[21]'s margin recipe based on the published data of inter- and intrafractional variability of tumor baseline shift.[7,8] The resulting total margins were 15.0-20.5 mm for the SI direction, 4.5-5.5 mm for the LR direction, and 7.5-10.0 mm for the AP direction.

Treatment planning and treatment setup

Multiplan (v. 4.0.x) was also used for treatment planning. The tracking method to be used for treatment correction was defined prior to plan optimization and dose calculation, in which case we used the XST mode.[22] In the XST mode, a region

of interest (ROI) that included a spine volume extending two vertebrae beyond the full PTV's length was defined. For each motion profile, we performed Monte Carlo dose optimization on the AVG images using two different collimators, one with a dimension comparable to the PTV's long axis and the other of a dimension that just matched the planning GTV (15 mm). For motion pattern #1, 20 and 35 mm circular collimators were chosen for treatment planning. For motion pattern #2, 20 and 40 mm collimators were used. For motion pattern #3, 20 and 35 mm collimators were chosen. In addition to the calculated ITV-to-PTV margins, we created two other plans with a fixed 5 mm ITV-to-PTV margin for a given motion profile (motion #3). This aimed to assess the sensitivity of dose received by the GTV to the ITV-to-PTV size. Therefore, a total of four treatment plans using 12.5, 20, 25, and 35 mm were created for motion #3. The Monte Carlo dose calculation algorithm of the MultiPlan TPS has been previously described by Ma *et al.*[23], and basically implements the MCDOSE, an EGS4 user code. All Monte Carlo dose calculations were performed at 0.5%-1% relative statistical uncertainty. The dose grid resolution was approximately 1.47 × 1.47 × 1.25 mm. Dose distributions were Gaussian-smoothed to reduce statistical noise. Total doses of 12.6 Gy in 3 fractions were prescribed to 65%-73% isodose lines (maximum dose = 100%) to achieve > 99% target coverage. Table 1 gives a summary of the final treatment plans. The fractioned dose was scaled to 4.2 Gy in order to accommodate the dose range applicable to the red channel of the Gafchromic EBT2 films.

Treatment setup was performed with the XST. Briefly, when the phantom loaded with the EBT2 films was placed on the treatment couch, stereoscopic kV image pairs were acquired and compared with synthetic DRRs computed a different angles in the predefined ROI of the spine structure by intensity-based 2D-3D registration [Figure 1].[9] The registration resulted in three translational and three rotational errors given as the differences of the spine structure between the treatment position and the planned position. These errors were subsequently corrected by movement of the treatment couch until the setup errors were reduced to less than 0.5 mm (translational) and 0.5° (rotational). The residual error for the spine alignment was then corrected by the CyberKnife robot and the treatment beams were delivered to the moving target according the spine-tumor relation from the planning CT.

We used an Epson Expression 1680 flatbed scanner (Seiko Epson Corporation, Nagano, Japan) to scan the exposed EBT2 films after post exposure ageing of 24 hours with the following settings: (1) transmission mode, (2) 48 bit color (RGB), (3) resolution of 150 dpi (0.017 cm/pixel), (4) no color correction, and (5) portrait orientation. EBT2 films were calibrated against measurements with an ion-chamber. The red-channel images of the EBT2 films were registered by the use of the Image Processing Toolbox™ of Matlab

Table 1: Summary of the treatment plans with listed values of minimum dose (D_{min}), mean dose (D_{mean}), and maximum dose (D_{max}) to the internal target volume

Motion	Collimator (mm)	D_{min} (Gy)	D_{mean} (Gy)	D_{max} (Gy)	HI
Motion #1 (10 mm in SI)	20	5.7	6.2	6.5	1.54
	35	5.0	5.4	6.0	1.43
Motion #2 (20 mm in SI,	20	4.5	5.3	6.0	1.43
5mm in AP, 2 mm in LR)	40	5.4	5.7	6.0	1.43
Motion #3 (10 mm in SI,	20	4.8	5.5	6.0	1.43
5 mm in AP, 2 mm in LR)	35	5.0	5.4	5.8	1.37
	12.5	4.3	5.3	6.1	1.47
	25	5.0	5.6	6.0	1.43

HI=Homogeneity index, LR=Left-right, SI=Superior-inferior

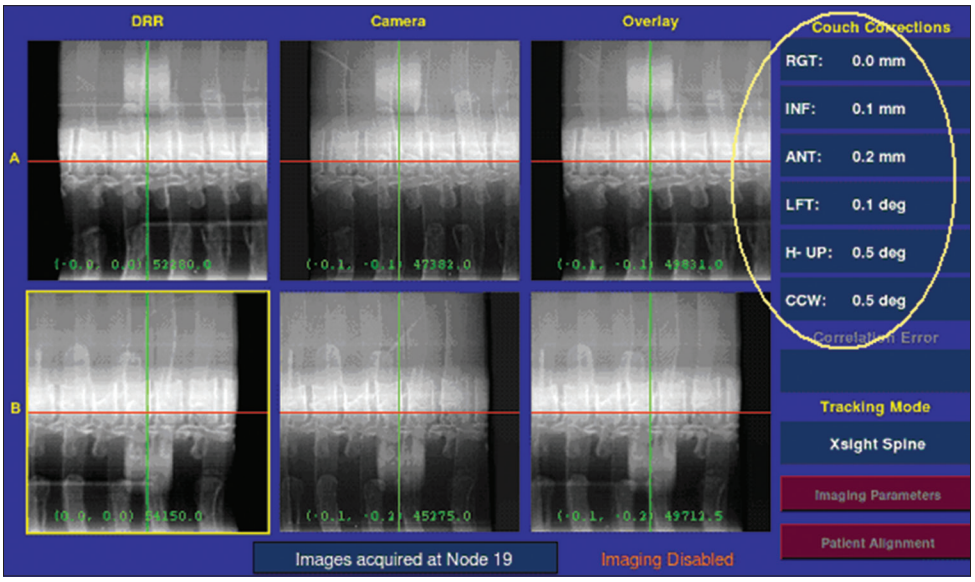

Figure 1: XSight Spine tracking registered the bony spine anatomy between the digitally reconstructed radiographs and the corresponding orthogonal stereoscopic images. The registration results, which are circled on the right, are three translational (left-right, superior-inferior and anterior-posterior) and three rotational errors (yaw, tilt, and roll). The shadow of the target appeared above (upper row) and beneath (bottom row) the spine structure

(The MathWork, Inc., Natick, MA, USA). We used an in-house Matlab program to analyze the dose distributions.

Dosimetric evaluations

Measured dose distributions were analyzed based on the percentage dose point that received a dose larger than the calculated prescription dose, minimum dose, and mean dose, denoted as $P_{>Dpres}$, $P_{>Dmin}$, and $P_{>Dmean}$, respectively. We used the coefficient of variation (CV) to evaluate the temporal dose variation. It is defined as

$$CV = \frac{\sigma}{\bar{d}} \times 100\%, \quad (1)$$

where σ is the standard deviation and $\bar{d}$ is the average dose in a single pixel over three fractions. A smaller CV indicated smaller dose variation in each pixel.

RESULTS

Figure 2 presents the cumulative dose distributions measured in the axial and coronal planes cutting through the GTV's center. Except the dose distribution obtained with the smallest 12.5 mm collimator, Figure 2 shows that all other measured dose distributions (in cGy) decreased from inside out, a pattern characteristic of the heterogeneous dose distribution with

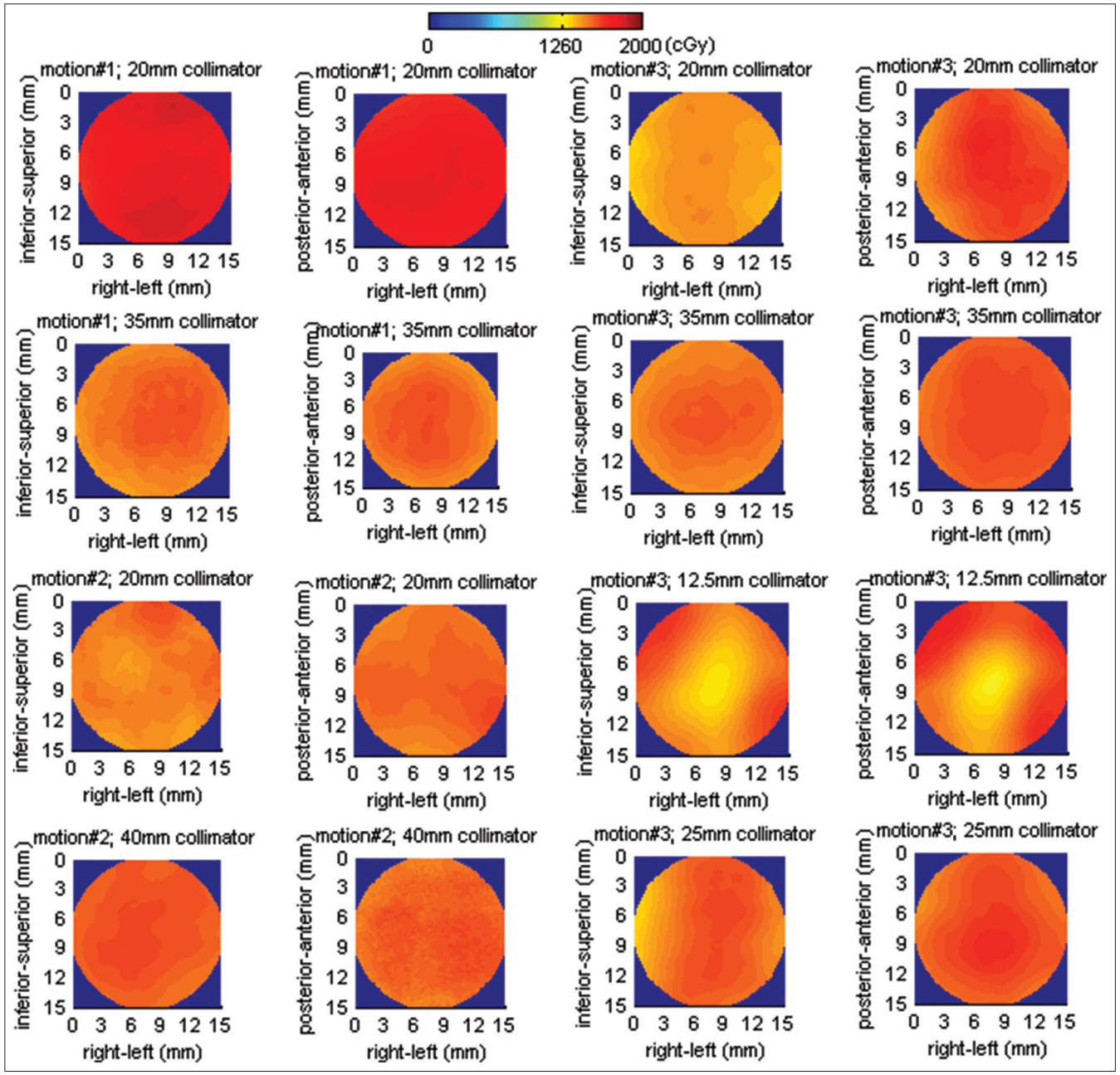

Figure 2: Cumulative dose distributions in the axial and coronal planes through the center of the gross tumor volume for different motion patterns and collimators. Doses are in cGy (see color bar)

larger collimators in SBRT. The cumulative dose distribution of the 12.5 mm collimator showed a reversed pattern in which the dose distribution was colder at the center characteristic of dose distributions for the CyberKnife with small collimators. More importantly, it demonstrates that the target attained the prescription dose of 12.6 Gy after the same plan was delivered three times, provided that the motion pattern remained constant from planning to delivery. Figure 3 illustrated the distributions of measured dose variations (1 SD) over three fractions in the axial and coronal films. Qualitatively, the dose variations tended to be greater in the coronal films than in the axial films. The dose variations were largest in the plan using 25 mm collimator for motion #3 and were smallest in the plan using 40 mm collimator for motion #2. In general, the dose variations differed from plan to plan without a clear pattern of correspondence to the composite dose distributions in Figure 2.

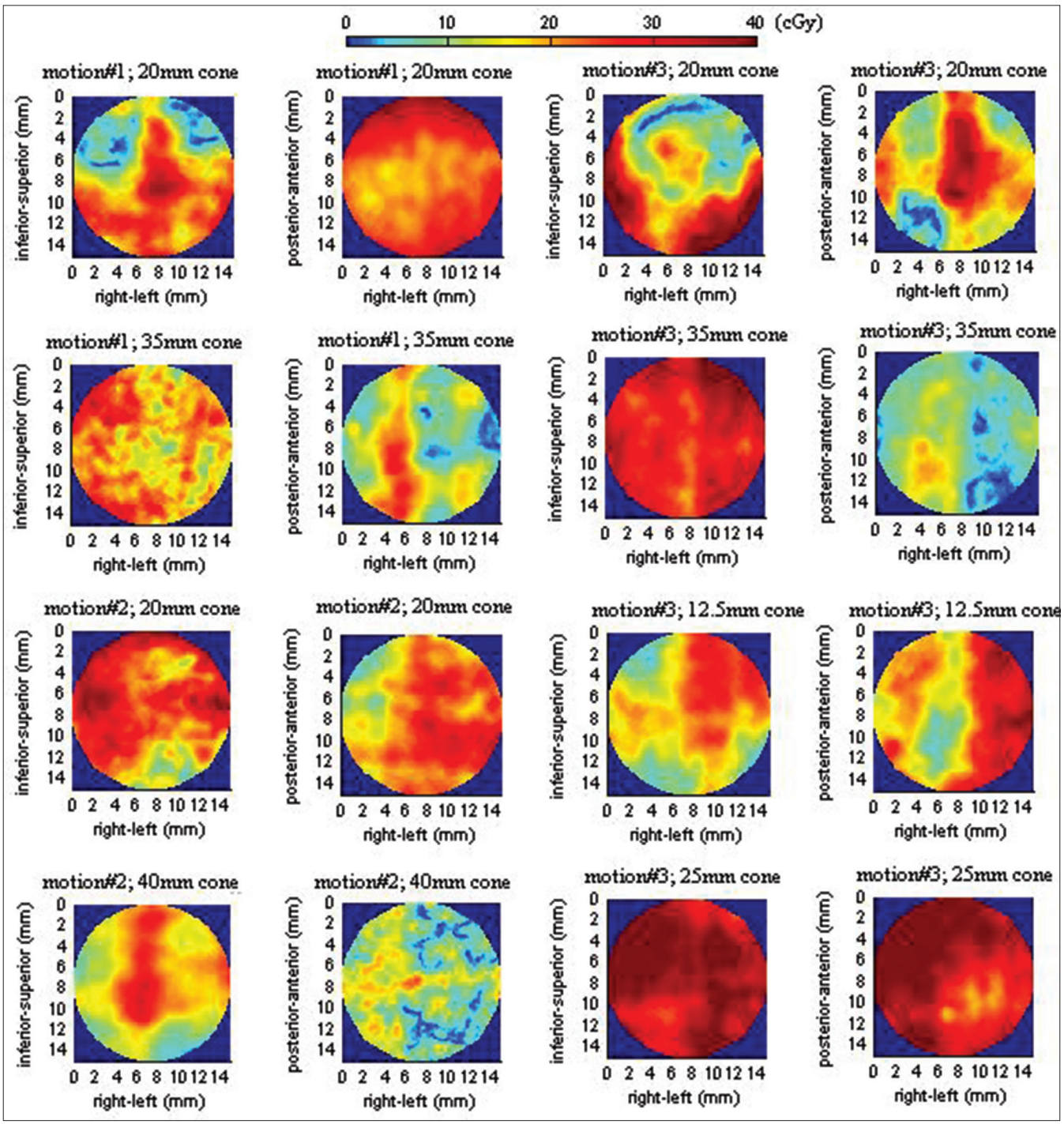

Figure 3: Distributions of the measured dose variations (1 standard deviation) in the coronal and axial planes of the moving target after the same treatment plans were delivered three times. Dose variations are in cGy (see color bar)

For quantitative analysis, we calculated the percentage of dose points exceeding the prescribed dose ($P_{>Dpres}$), the calculated minimum dose ($P_{>Dmin}$), and the calculated mean dose ($P_{>Dmean}$) as a function of the motion pattern [Table 2]. Table 2 shows that $P_{>Dpres}$ was < 100% for only a few single fractions, but the cumulative $P_{>Dpres}$ approached 100% in all treatments. In contrast, the values of $P_{>Dmin}$ and $P_{>Dmean}$ were seen to differ significantly between fractions. For example, $P_{>Dmin}$ can vary from ~ 25% in the first fraction to ~ 2% in the remaining fractions and ends up ~ 0% after three fractions. The cumulative $P_{>Dmin}$ ranged from 0% to 99.4% (74.9 ± 33.5% [mean ± 1 standard deviation]). The cumulative $P_{>Dmean}$ were <5% except for the plans using the 12.5 mm collimator. Figure 4 showed the histograms of the CV for each motion profile. The average CV for all dose points is shown in the CV histograms for different collimators. For motion #1, the CV ranged from 0.02% to 7.53%, whereas for motion #2, the CV ranged from 0.03% to 8.90%, and last, for motion #3, the CV ranged from 0.01% to 11.80% for a normal ITV-to-PTV margin and from 0.59% to 11.85% for a reduced margin.

Results of the Mann-Whitney U tests showed that $P_{>Dpres}$, $P_{>Dmean}$, and $P_{>Dmin}$ were insensitive to the margin size ($P > 0.05$), at least for a 3D translational motion of clinically relevant amplitude (e.g., SI = 10mm, AP = 5mm, and LR = 2mm). The Spearman's rank correlation coefficients between $P_{>Dpres}$, $P_{>Dmean}$, and $P_{>Dmin}$ and collimator size were $r = 0.39$, -0.56, and - 0.49, respectively. The correlation coefficients were significant for $P_{>Dmean}$ and $P_{>Dmin}$ ($P < 0.05$) but not $P_{>Dpres}$ ($P > 0.05$).

DISCUSSION

In this study, we investigated the feasibility of highly conformal stereotactic body radiation therapy (SBRT) by using CyberKnife for lung tumors that are attached to the rigid spine structure and exhibit small motion. This strategy adapted the XSight Spine Tracking system (XST) for setup correction and employed individualized internal target volumes (ITV) with an additional margin for inter- and intrafractional variability of the tumor baseline. The dosimetric impact of such treatment strategy for SBRT was evaluated with Gafchromic EBT2 films in a lung phantom consisting of a moving target and a static spine structure. Assuming constant target motion during 4DCT scanning and delivery, our results showed that the gross target volume (GTV) received the prescription dose after three fractions despite a marked temporal dose variation. No serious impact of tumor control probability is expected because the cumulative $P_{>Dpres}$ was 100% for all plans, even though it can be smaller (~96%) in a single fraction. On the contrary, values of $P_{>Dmean}$ for each fraction and after three fractions were < 5% for all plans except one, suggesting that the overall effect of target motion was decreasing the delivered dose [Figure 3]. In practice, values of $P_{>Dpres}$, $P_{>Dmean}$, and $P_{>Dmin}$ primarily depended on the planned dose to the ITV and did not differ by margin size, because with only periodic motion the idealized 5 mm margin was enough to compensate

Table 2: Percent dose points that have measured dose values larger than the prescription dose ($P_{>Dpres}$), mean dose ($P_{>Dmean}$), and minimum dose ($P_{>Dmin}$) were calculated for each fraction and were averaged over three fractions. Also, given are the coefficients of variation

Motion	Fraction no.	$P_{>Dpres}$	$P_{>Dmin}$	$P_{>Dmean}$	CV
Motion #1					
20 mm collimator	1	100.0	85.0	0.0	
	2	100.0	77.2	1.7	
	3	100.0	71.1	9.6	
	Cumulative	100.0	89.1	0.0	3.7
35 mm collimator	1	100.0	72.6	7.8	
	2	100.0	40.3	0.0	
	3	100.0	73.8	7.6	
	Cumulative	100.0	62.7	0.0	3.2
Motion #2					
20 mm collimator	1	100.0	99.2	0.0	
	2	100.0	100.0	34.1	
	3	100.0	100.0	13.1	
	Cumulative	100.0	100.0	3.5	4.6
40 mm collimator	1	100.0	25.5	1.1	
	2	100.0	1.9	0.0	
	3	100.0	1.7	0.0	
	Cumulative	100.0	0.0	0.0	2.8
Motion #3					
20 mm collimator	1	98.4	53.5	0.1	
	2	100.0	67.1	6.5	
	3	100.0	80. 5	22.6	
	Cumulative	100.0	67.7	4.6	3.8
35 mm collimator	1	100.0	100.0	0.1	
	2	100.0	99.7	0.0	
	3	100.0	63.1	0.0	
	Cumulative	100.0	99.4	0.0	3.8
12.5 mm collimator	1	97.4	94.8	24.6	
	2	97.8	94.7	9.4	
	3	100.0	99.5	31.0	
	Cumulative	100.0	99.0	20.1	4.0
25 mm collimator	1	96.5	12.0	0.0	
	2	100.0	95.7	25.7	
	3	100.0	85.9	6.8	
	Cumulative	100.0	80.9	0.1	7.0

CV=Coefficient of variation

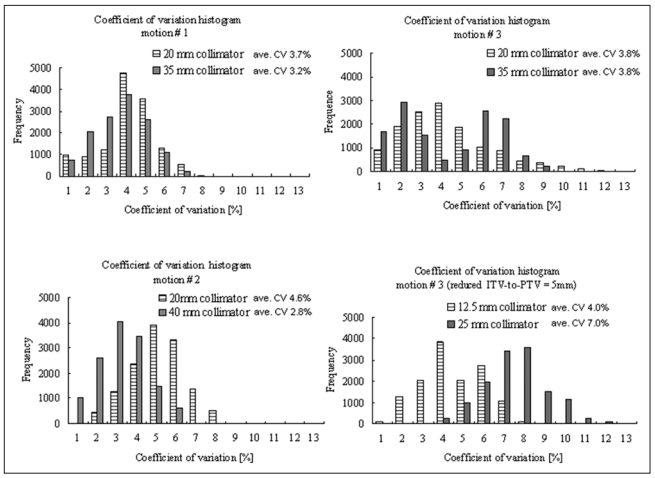

Figure 4: Coefficient of variation histograms for all motion patterns with different collimator sizes. Average coefficient of variation values are given on the histograms as "ave. coefficient of variation"

for the dose blurring at the planning target volumes (PTV) edge. Nonetheless, strong temporal dose variations were evidenced in the histogram plots of the CV [Figure 4]. The average CV was ~ 3.5% for small motion (10 mm SI motion) and up to 7.0% for large SI motion (20 mm) with a reduced 5 mm ITV-to-PTV margin. In an experimental study, Jiang *et al.*,[14]found negligible dose variation of 1%-2% in a chamber measurement that was made in a moving phantom after 30 fractions, independent of the MLC delivery mode. In the other study, Ehler *et al*.[24] found a CV of 1.14%-5.51% in segment IMRT and 3.83%-8.25% in dynamic IMRT in measurements that were made with a moving detector array. Due to variations of phantom setup (e.g. homogeneous vs. heterogeneous phantom), dose calculation algorithms (e.g. Monte Carlo vs. pencil beam) and fractionation schemes, direct comparisons between the results of these studies are difficult. In our case, the increased dose variations can be explained by the large dose gradients (e.g. 27%~35%) inside the PTV. This was in contrast to conventional 3D conformal radiotherapy and IMRT, where the effect of target motion is generally pronounced at the field edge, but negligible at the center of the uniform field.

In SBRT, fractioned doses are up to 15-20 Gy, -3-4.5 times that of this study. If we were to deliver 20 Gy, the dose per fraction and hence the number of monitor units per beam would be roughly scaled up 4.5 times accordingly. This may have some impact on the resulting dose because the larger the number of monitor units (i.e., longer treatment time), the higher the probability of the target will be sampled by the treatment beams. The reduced dose error with larger number of monitor units has been recently examined by Ong *et al.*[25] in multileaf collimator-based hypofractionated stereotactic lung radiotherapy. Because issues with MLC may not be strictly relevant to the robotic-based IMRT, more studies are necessary for understanding how these factors influence the delivered dose in the present robotic-based treatment scenario.

One of the limitations of this study is the relatively large target-to-spine distance in the phantom as this technique is aimed for tumors in the immediate vicinity of the spinal column. However, we do not expect that the results would be affected by the target-to-spine distance because of the constant and regular target motion and the overall rigidness of the phantom. Nevertheless, intrafractional and interfractional variability of tumor motion range, period and baseline are noted frequently in lung radiotherapy.[7,26] Although we explicitly calculated the extra setup margins for these uncertainties, we were unable to assess their dosimetric effects with the present experimental setup. It is expected that increased inter- and intrafractional tumor baseline drifts relative to the tracking spine volume may increase the delivered dose errors. Huang *et al*.[13] recently showed that treatment plans created with inaccurate ITV led to underdosing (10%) in a portion of the PTV when the irregular target motion was large (~20 mm), whereas good agreement between planned and measured dose distributions was observed for irregular motion <8.8 mm. This seemed to be consistent with our preliminary results that measured minimum and mean doses tended to decrease with increasing motion amplitude (10 mm *vs.* 20 mm).

Because XST represents an offline treatment setup strategy, it is impossible to reduce the setup margin. Yet, there is great potential to reduce the internal margin despite non-real-time tracking. Murphy *et al*.[27] have demonstrated the effectiveness of breath-holding to reduce and stabilize the tumor motion in hypofractionated radiotherapy. A major concern of such breath-held approach is prolonging the treatment duration beyond the patient's compliance. Recently, the concept of time-weighted average tumor position has been proposed by Wolthaus *et al*.[21] Unlike the concept of ITV which aims to provide 100% dose coverage to the clinical target volume (CTV) during the entire breathing cycle, Wolthaus *et al*.[21] suggested that, if a treatment plan is designed for the tumor at its time-weighted average position during the breathing cycle, a good dose coverage is still obtained even though the target is not fully within the PTV during a short portion of the breathing cycle. Guckenberger *et al*.[28] estimated that 2.4 and 6 mm margins around the CTV at the time-weighted average position were needed to compensate for motion amplitudes of 10 and 20 mm. This nearly halves the internal margin. If such margin design is adapted to treatment planning of our proposed strategy, it may be possible to reduce the total safety margin from 15.2 to 11.9 mm and 20.7 to 15.1 mm for motion amplitudes of 10 and 20 mm. In addition, stereoscopic images do not provide volumetric information about changes in tumor volume that has been noted by Britton *et al*.[29] It is important to repeat 4DCT simulation to confirm that there is no continuous progressive change in tumor volume and position, particularly for hypofractionated/accelerated regimens that take a few weeks to complete.

CONCLUSIONS

For the first time, a quantitative dosimetric evaluation of target motion in robotic hypofractionated delivered using the XSight Spine Tracking method was performed. Although the target received the prescription dose after three fractions, this technique should be used with caution because the temporal dose variations can be significant. Unless effective means are employed to reduce the safety margin and variability of tumor motion, we do not recommend the non-real-time spine tracking strategy for treating tumors with motion of more than 10 mm. Finally only long term clinical evaluation of this method will demonstrate efficacy of this treatment strategy.

REFERENCES

1. Brown WT, Wu X, Fayad F, Fowler JF, Amendola BE, Garcia S, *et al*. CyberKnife Radiosurgery for Stage I Lung Cancer: Results at 36 months. Clin Lung Cancer 2007;8:488-492.
2. Unger K, Ju A, Oermann E, Suy S, Yu X, Vahdat S, *et al*. CyberKnife for hilar lung tumors: Report of clinical response and toxicity. J Hematol Oncol 2010;3:39.

3. Bibault J-E, Prevost B, Dansin E, Mirabel X, Lacornerie T, and Lartigau E. Image-guided robotic stereotactic radiation therapy with fiducial-free Tumor tracking for lung cancer. Radiat Oncol 2012;7:102.
4. Schweikard A, Shiomi H, and Adler J. Respiration tracking in radiosurgery. Med Phys 2004;31:2738-2741.
5. Reichner CA, Collins BT, Gagnon GJ, Maliks S, Jamis-Dow C, and Anderson ED. Comparison of fiducial placement for Cyberknife stereostatic radiosurgery using CT-guidance or flexible bronchoscopy. Chest 2005;128:162-163S.
6. Strulik KL, Cho MH, Collins BT, Khan N, Banovac F, Slack R, *et al*. Fiducial migration following small peripheral lung tumor image-guided CyberKnife stereotactic radiosurgery. Medical Imaging 2008: Visualization, Image-Guided Procedures, and Modeling 2008;6918:69181A-69181A-9.
7. Sonke J-J, Lebesque J, and Vanherk M. Variability of four-dimensional computed tomography patient models. Int J Radiat Oncol Biol Phys 2008;70:590-598.
8. Worm ES, Hansen AT, Petersen JB, Muren LP, Præstegaard LH, and Høyer M. Inter- and intrafractional localisation errors in cone-beam CT guided stereotactic radiation therapy of tumours in the liver and lung. Acta Oncol 2010;49:1177-1183.
9. Ho AK, Fu D, Cotrutz C, Hancock SL, Chang SD, Gibbs IC, *et al*. A study of the accuracy of Cyberknife spinal radiosurgery using skeletal structure tracking. Neurosurgery 2007;60:147-156.
10. Bortfeld T, Jokivarsi K, Goitein M, Kung J, and Jiang SB. Effects of intra-fraction motion on IMRT dose delivery: Statistical analysis and simulation. Phys Med Biol 2002;47:2203-2220.
11. Richter A, Wilbert Jr, and Flentje M. Dosimetric evaluation of intrafractional tumor motion by means of a robot driven phantom. Med Phys 2011;38:5280.
12. Nakamura M, Miyabe Y, Matsuo Y, Kamomae T, Nakata M, Yano S, *et al*. Experimental validation of heterogeneity-corrected dose-volume prescription on respiratory-averaged CT images in stereotactic body radiotherapy for moving tumors. Med Dosim 2012;37:20-25.
13. Huang L, Park K, Boike T, Lee P, Papiez L, Solberg T, *et al*. A study on the dosimetric accuracy of treatment planning for stereotactic body radiation therapy of lung cancer using average and maximum intensity projection images. Radiother Oncol 2010;96:48-54.
14. Jiang S, Pope C, Al Jarrah K, Kung J, Bortfeld T, and Chen G. An experimental investigation on intra-fractional organ motion effects in lung IMRT treatments. Phys Med Biol 2003;48:1773-1784.
15. Ong C, Verbakel WFAR, Cuijpers JP, Slotman BJ, and Senan S. Dosimetric impact of interplay effect on RapidArc lung stereotactic treatment delivery. Int J Radiat Oncol Biol Phys 2010;79:305-311.
16. Chan MKH, Kwong DLW, Ng SCY, Tong ASM, and Tam EKW. Experimental evaluations of the accuracy of 3D and 4D planning in robotic tracking stereotactic body radiotherapy for lung cancers. Med Phys 2013;40:041712.
17. Chan MKH, Kwong DLW, Ng SCY, Tong ASM, and Tam EKW. Accuracy and sensitivity of four-dimensional dose calculation to systematic motion variability in stereotatic body radiotherapy (SBRT) for lung cancer. J Appl Clin Med Phys 2012;13:303-317.
18. Bahig H, Campeau M-P, Vu T, Doucet R, Béliveau Nadeau D, Fortin B, *et al*. Predictive parameters of CyberKnife fiducial-less (XSight Lung) applicability for treatment of early non-small cell lung cancer: A single-center experience. Int J Radiat Oncol Biol Phys 2013;87:583-589.
19. Dieterich S and Suh Y, Tumor motion ranges due to respiration and respiratory motion characteristics, in Treating Tumors that Move with Respiration, H. Urschel, Jr., Kresl J, Luketich J, Papiez L, Timmerman R, Schulz R, Editors. 2007, Springer Berlin Heidelberg. p. 3-13.
20. Lamond J, Weiner J, Oliai C, Lanciano R, Yang J, Brady L, Comparison of stereotactic body radiation therapy results for clinical stage 1 non-small cell lung cancer using 3 different tracking modalities, in The SRS/SBRT Scientific Meeting 2013: Carlsbad, CA.
21. Wolthaus J, Sonke J-J, Vanherk M, Belderbos J, Rossi M, Lebesque J, *et al*. Comparison of different strategies to use four-dimensional computed tomography in treatment planning for lung cancer patients. Int J Radiat Oncol Biol Phys 2008;70:1229-1238.
22. Fürweger C, Drexler C, Kufeld M, Muacevic A, Wowra B, and Schlaefer A. Patient motion and targeting accuracy in robotic spinal radiosurgery: 260 single-fraction fiducial-free cases. Int J Radiat Oncol Biol Phys 2010;78:937-945.
23. Ma CM, Li JS, Deng J, and Fan J. Implementation of Monte Carlo dose calculation for CyberKnife treatment planning. J Phys Conf Ser 2008;102:012-016.
24. Ehler ED, Nelms BE, and Tomé WA. On the dose to a moving target while employing different IMRT delivery mechanisms. Radiother Oncol 2007;83:49-56.
25. Ong CL, Dahele M, Cuijpers JP, Senan S, Slotman BJ, and Verbakel WFAR. Dosimetric impact of intrafraction motion during RapidArc stereotactic vertebral radiation therapy using flattened and flattening filter-free beams. Int J Radiat Oncol Biol Phys 2013;86:420-425.
26. Seppenwoolde Y, Shirato H, Kitamura K, Shimizu S, van Herk M, Lesbesque JV, *et al*. Precise and real-time measurement of 3D tumor motion in lung due to breathing and heartbeat, measured during radiotherapy. Int J Radiat Oncol Biol Phys 2002;53:822-834.
27. Murphy MJ, Martin D, Whyte R, Hai J, Ozhasoglu C, and Le Q-T. The effectiveness of breath-holding to stabilize lung and pancreas tumors during radiosurgery. Int J Radiat Oncol Biol Phys 2002;53:475-482.
28. Guckenberger M, Krieger T, Richter A, Baier K, Wilbert J, Sweeney RA, *et al*. Potential of image-guidance, gating and real-time tracking to improve accuracy in pulmonary stereotactic body radiotherapy. Radiother Oncol 2009;91:288-295.
29. Britton KR, Starkschall G, Tucker SL, Pan T, Nelson C, Chang JY, *et al*. Assessment of gross tumor volume regression and motion changes during radiotherapy for non–small-cell lung cancer as measured by four-dimensional computed tomography. Int J Radiat Oncol Biol Phys 2007;68:1036-1046.

Cite this article as: Chan MK, Kwong DL, Lee VW, Leung RW, Wong MY, Blanck O. Feasibility study of robotic hypofractionated lung radiotherapy by individualized internal target volume and XSight Spine Tracking: A preliminary dosimetric evaluation. J Can Res Ther 2015;11:150-7.

Source of Support: Nil, **Conflict of Interest:** None declared.